31st International Conference Nuclear Energy for New Europe
NENE 2022 September 12-15 PORTOROŽ SLOVENIA

Development of a 3D-RPV Finite Element Model for Pressurized Thermal Shock Analyses

Oriol Costa Garrido[1], Nejc Kromar[1,2], Andrej Prošek[1], Leon Cizelj[1]
[1]Jožef Stefan Institute, Jamova cesta 39
[2]Faculty of Mechanical Engineering, University of Ljubljana, Aškerčeva 6
[1,2]SI-1000 Ljubljana, Slovenia
oriol.costa@ijs.si, nejckromar@gmail.com, andrej.prosek@ijs.si, leon.cizelj@ijs.si

ABSTRACT

This paper presents the development of a full three-dimensional (3D) finite element model of a reactor pressure vessel (RPV). The goal is to generate the model meshes required to accurately analyse the temperatures and stresses developing in the RPV during a small-break loss-of-coolant accident (SB-LOCA). To that end, several meshes are developed with different element densities. The inner surface of the RPV is assumed to be subjected to time-dependent and uniformly-distributed fluid temperature, heat-transfer coefficient and pressure representative of the SB-LOCA transient. These same loads are used in a parallel analysis with the FAVOR code, which assumes a 1D model (in the through-thickness radial direction) of the RPV wall. The results obtained with the developed meshes and the FAVOR code are then compared. The outcomes of the comparison include the selected mesh for accurate results and reasonable computational resources to perform the analyses, as well as the impact on the results from the use of 1D and 3D RPV wall models.

1 INTRODUCTION

The reactor pressure vessel (RPV) is an indispensable component in nuclear power plants and its structural integrity must be assured under all possible events. The limiting event for the long-term operation (LTO) of the RPV is the pressurized thermal shock (PTS) [1]. A PTS event typically follows a loss-of-coolant accident (LOCA), or other emergency scenarios, where the subsequent injection of cold water from the emergency core cooling system into the hot RPV may induce high thermal stresses in the RPV wall. The RPV wall material undergoes neutron embrittlement after several years of operation, with the subsequent hardening and loss of fracture toughness. PTS analyses are thus needed to assure that a potentially existing flaw in the RPV wall will not initiate and propagate rapidly in a brittle-fracture manner during emergency scenarios.

One of the main goals of the European project APAL (Advanced PTS Analysis for LTO) is the development of advanced, deterministic and probabilistic, PTS assessment methods [2]. Within APAL, benchmark calculations will be performed to address multidisciplinary and multi-physics challenges related to the integrity assessment of RPV under PTS events. To that end, a small-break loss-of-coolant accident (SB-LOCA) has been simulated within the project in order to produce relevant sets of thermal-hydraulic outputs to be used in the structural assessment. The APAL PTS transient is described in Section 2, and Section 3 presents the development of the finite element model (FEM) of the APAL three-dimensional (3D) RPV. Several meshes are generated and the analyses in Section 4 compare the results of the 3D RPV

with those produced with the FAVOR (Fracture Analysis of Vessels – Oak Ridge) code [3]. Finally, the conclusions are drawn in Section 5.

2 PTS EVENT

A 4-loops Kraftwerk Union KWU-1300 pressurized water reactor (PWR) – Konvoi German design – plant has been selected for the studies within the APAL project. The selected emergency scenario leading to a PTS event is a SB-LOCA from a 50 cm^2 break in the hot leg (HL) of loop #1 together with loss of offsite power. The high-pressure safety injection (HPSI) trains in loop #1 and #4 are assumed to be, respectively, down for maintenance and to fail at the start of the transient. Therefore, only loops #2 and #3 receive emergency core cooling water from the high-pressure pumps. However, all four loops receive injection from the low-pressure safety injection (LPSI) pumps. The four accumulators (ACCs) connected to cold legs (CLs) are active while the four accumulators connected to HLs are deactivated. Thus, the APAL transient outputs approximate the thermal-hydraulic data used in the International Comparative Assessment Study (ICAS) project for transient T2 [4]. The outputs of the thermal-hydraulic analyses with the RELAP5 code [5] at the beltline weld elevation of 2638 mm below the CL3 nozzle centerline (with HPSI) shown in Figure 1 are employed as inputs in the structural analyses. These include the fluid temperature, pressure and heat transfer coefficient (HTC). Note that the thermal-hydraulic analyses in APAL have been performed by several partners with different computer codes for a transient length of 5000 s and extended to 10000 s [6]. The analyses presented here are limited to 3000 s as this time is sufficient for the development of the structural model.

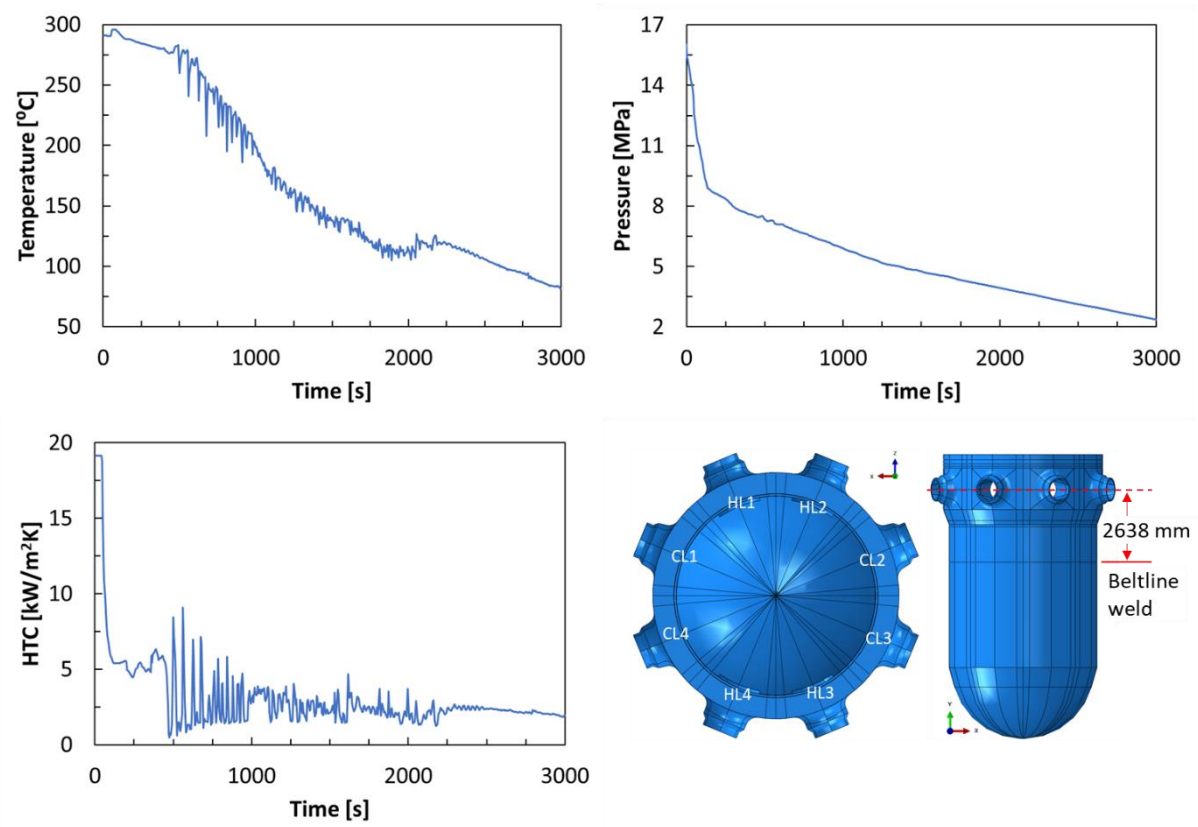

Figure 1: Fluid temperature, heat transfer coefficient and pressure from the SB-LOCA transient, used as thermal and mechanical loads in the structural analyses

3 RPV STRUCTURAL MODEL

Relevant dimensions of the KWU-1300 RPV include the inner and outer radii of r_i = 2435 mm and r_o = 2684 mm, respectively, in the cylindrical part of the RPV. The wall thickness consists of a 6 mm austenitic-steel cladding and 243 mm ferritic-base material. The border between both materials is named here as fusion line (fl). The temperature-dependent properties of both materials given in Table 1 are considered in the analyses.

Table 1: Physical and mechanical properties of the RPV materials

Material	**Ferritic low-alloy steel (base)**					**Austenitic steel (cladding)**				
Temperature [°C]	20	100	200	300	350	20	100	200	300	400
Young's modulus [GPa]	206	199	190	181	172	200	194	186	179	172
Poisson's ratio [-]	0.3									
Th.Conductivity [W/mK]	44.4	44.4	43.2	41.8	39.4	16.0	16.0	17.0	17.0	18.0
Spec. Heat capacity [J/gK]	0.45	0.49	0.52	0.56	0.61	0.50	0.50	0.54	0.54	0.59
Mean Th.Ex.Coef. $x10^{-6}$ [1/K]	10.3	11.1	12.1	12.9	13.5	15.0	16.0	17.0	19.0	21.0
Stress free temperature [°C]	291									
Density [kg/m^3]	7800									

Five model meshes of the RPV shown in Figure 2 and described in Table 2 have been developed assuming different element densities and interpolation orders. Note that linear and quadratic elements are used in meshes 3 and 3q, respectively. Uncoupled heat-transfer (HT) and mechanical (MC) analyses are performed with the 5 model meshes. In the HT analyses, the fluid temperature and HTC in Figure 1 are assumed to be uniformly distributed at the inner surface of the RPV. The obtained RPV wall temperatures are then used as thermal loads in the subsequent MC analyses, where a uniformly distributed pressure load (Figure 1) is additionally acting on the inner surface. The boundary conditions shown in Figure 2 (top-right) are applied on the top surface of the RPV to avoid free-body movement while allowing free-uniform deformation in the radial direction. These boundary conditions include zero displacement in vertical direction of the upper surface (Uy=0), and the edges parallel to x and z directions have zero displacements in z (Uz=0) and x (Ux=0) directions, respectively. The initial 3000 seconds of the transient are used in the time-dependent structural analyses and the RPV wall temperatures and stresses are obtained every 3 seconds.

Table 2: Description of meshes used in the sensitivity analysis

Mesh	**Element order**	**Number of elements in cladding thickness**	**Total number of elements**	**Total number of nodes**	**Total CPU TIME [h]**	
					HT	**MC**
1	Linear	4	397344	442394	47	61
2		4	186816	208058	9	23
3		1	119232	138319	14	12
3q	Quadratic	1	119232	534053	29	201
4		2	138688	613015	35	268

The uniform load distribution at the inner surface of the 3D-RPV allows for a fair comparison of the analysis results with those obtained with the FAVOR code [3]. The FAVOR code has been specifically developed to perform integrity analyses of RPV under PTS, and it

employs an axisymmetric 1D simplification of the RPV wall in the thickness (radial) direction. Thus, the 1-point thermal-hydraulic data in Figure 1 is also employed as inputs in the FAVOR calculations.

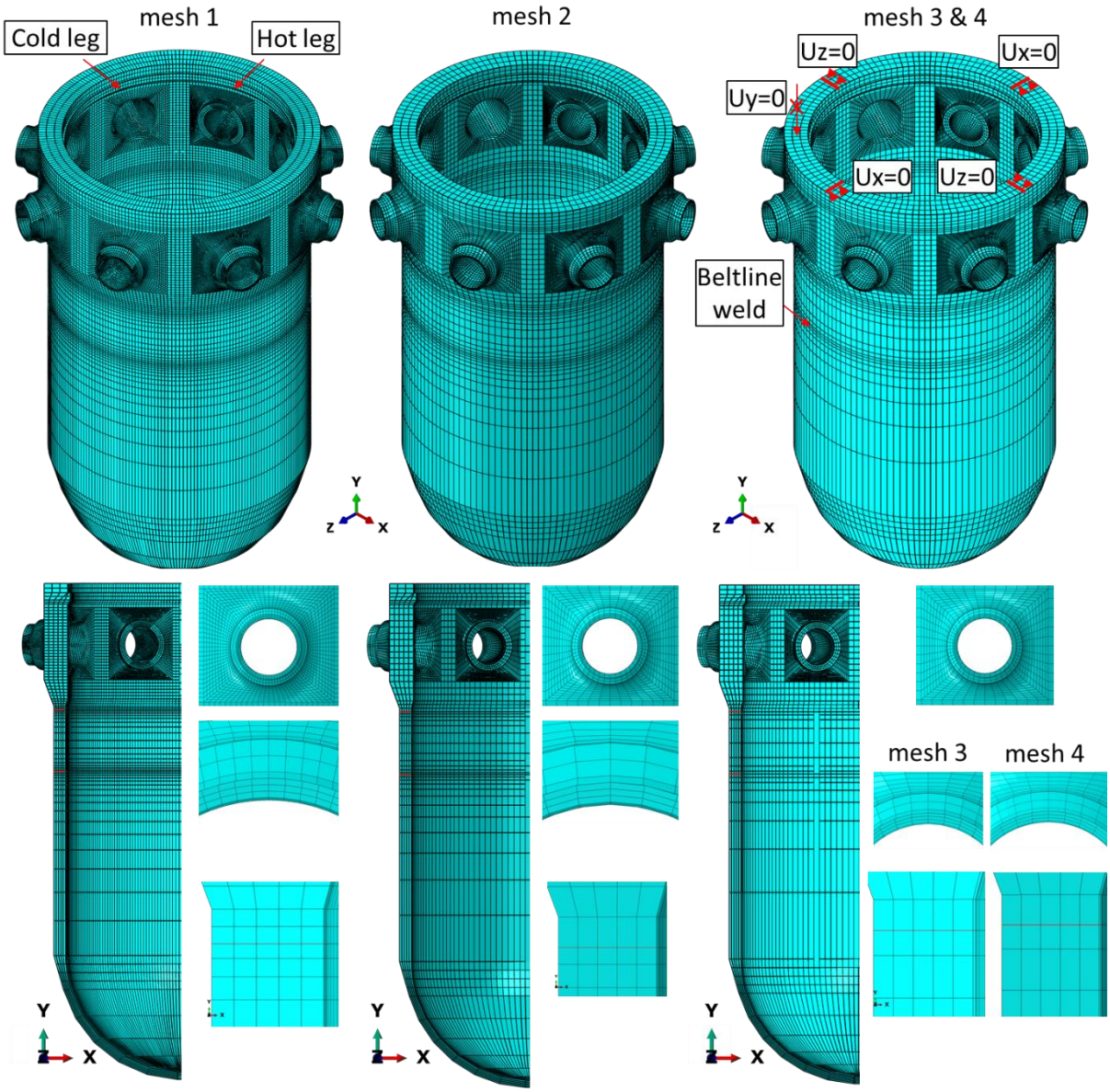

Figure 2: Finite element model meshes of the RPV

4 ANALYSIS RESULTS

This section presents the thermo-mechanical analysis results with the 3D-RPV model and the FAVOR code. The results with the 3D-RPV model are studied at the beltline weld elevation of 2638 mm below the CL3 nozzle centerline (see Figure 1). The obtained temperatures and stresses that develop in the RPV during the PTS event are first presented, followed by the mesh sensitivity analysis of the 3D-RPV model.

4.1 PTS EVENT RESULTS

Figure 3 presents the results obtained with mesh 4 (Table 2) and the FAVOR code regarding temperatures, hoop (S_h) and axial (S_a) stresses at the inner (r_i) and outer (r_o) surfaces. For the stresses, the results are also shown at the fusion line (fl) between the cladding and base materials. Note that stresses at the fusion line are discontinuous with different values at both materials. Therefore, the fusion-line stresses are reported as the average of the cladding and base values, which are represented as $<S_h(fl)>$ and $<S_a(fl)>$ for the hoop and axial components, respectively.

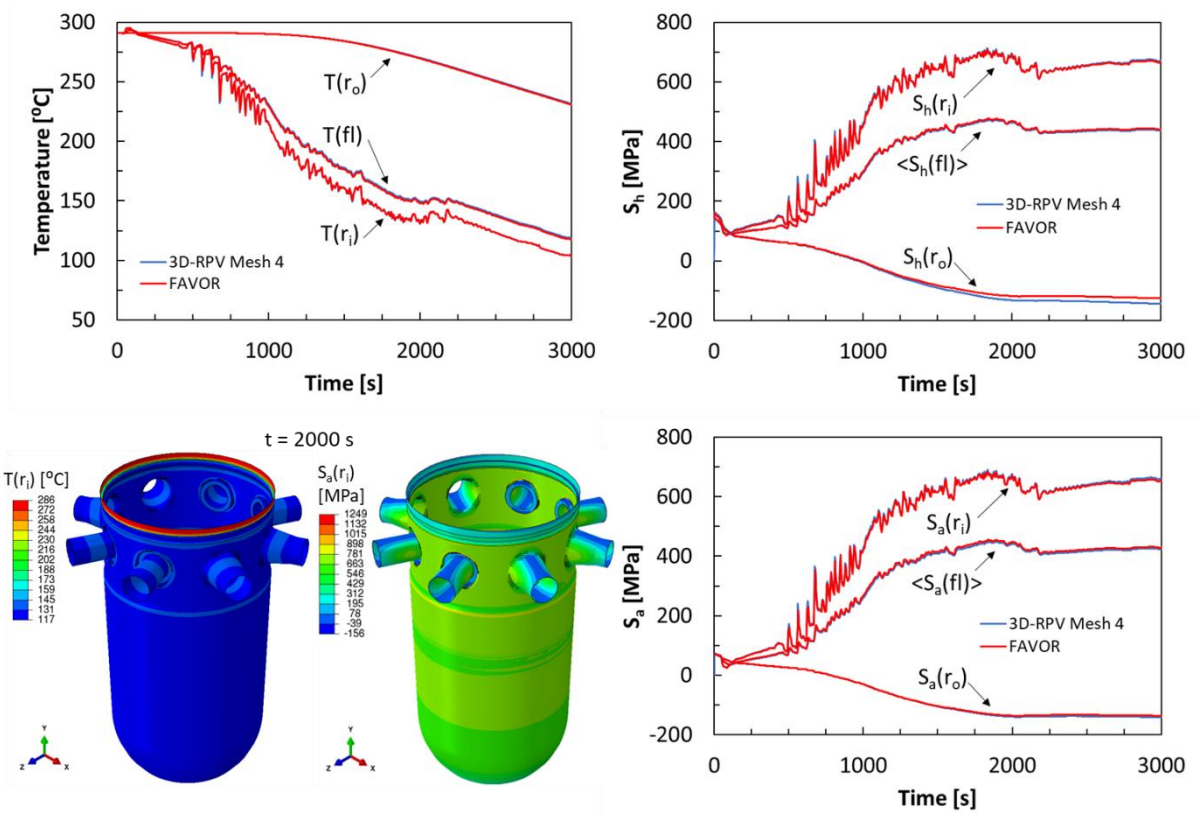

Figure 3: Comparison of thermo-mechanical results between mesh 4 and FAVOR

It can be observed in Figure 3 that the FAVOR code yields very similar results as those obtained with the 3D-RPV at the beltline weld elevation below CL3. This indicates that the 1D RPV simplification implemented in FAVOR yields correct results at this location, as it is in the middle of the cylindrical part of the RPV and due to the uniform-load assumption.

Figure 3 also shows the typical results' pattern in PTS analyses. At the beginning of the transient, rather low tensile stresses are present due to pressure load. The stresses initially decrease due to the initial fast depressurization of the system. This is then followed by a fast increase of the inner surface stresses (now mostly of thermal nature) induced by the existing thermal gradients in the RPV wall thickness. Indeed, due to the injection of cold emergency water, the inner surface temperatures quickly decrease while the outer surface temperatures remain high. At the same time, the outer surface stresses become compressive.

4.2 RESULTS OF THE MESH SENSITIVITY

Figure 4 shows the comparison of the relative differences with respect to mesh 4 of the results with all other meshes and FAVOR. Note that the mesh 4 results are taken as reference since this quadratic mesh contains the highest number of nodes, and thus, degrees of freedom (Table 2).

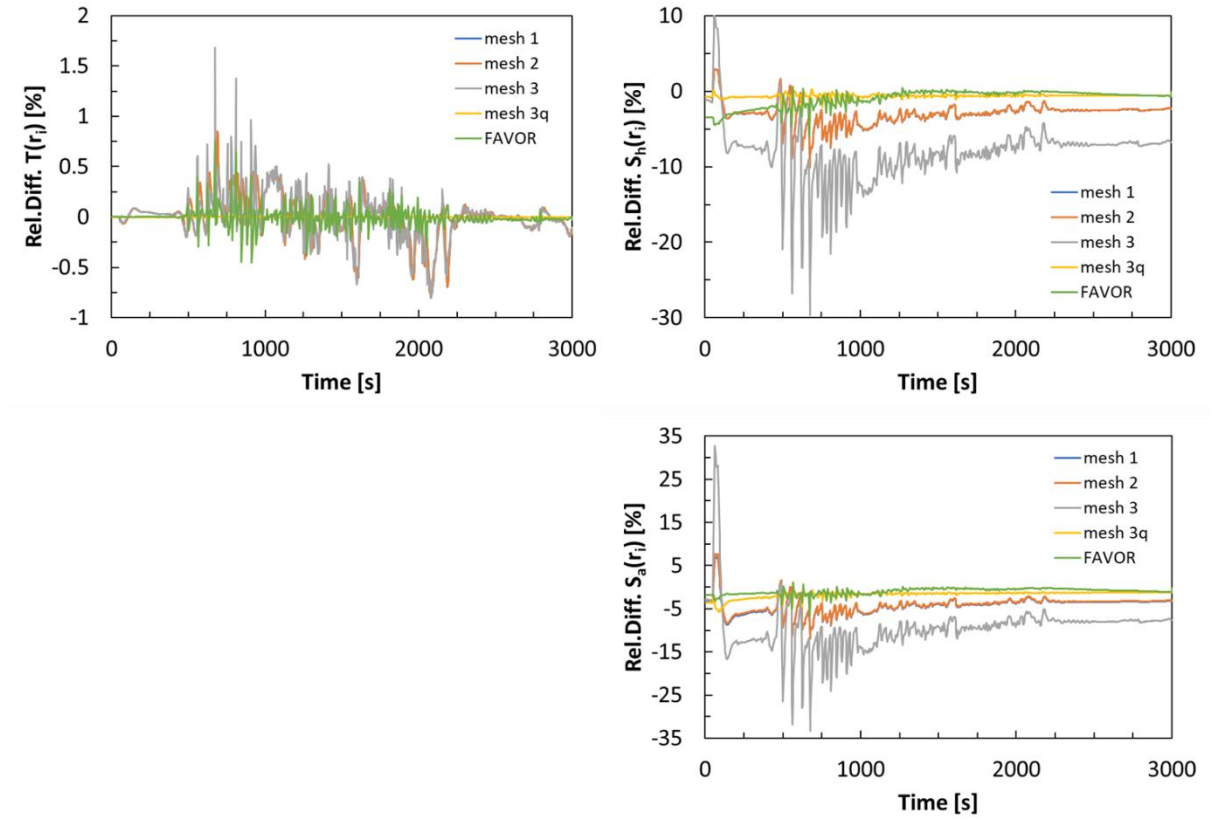

Figure 4: Relative difference of results from different meshes and FAVOR with respect to results from mesh 4

The results in Figure 4 show that the inner surface temperature is well captured with all meshes and FAVOR, as they all fall within the ~ (-1%, +2%) interval when compared to mesh 4. However, this observation changes when it comes to stress results, as those obtained with linear meshes (1, 2 and 3) are clearly offset. Results with quadratic mesh 3q and FAVOR can be seen to be in a rather good agreement with mesh 4. Observing the qualitative and quantitative differences between mesh 3 and mesh 3q results, the latter in strong agreement with mesh 4 and FAVOR, highlights the importance of using quadratic elements in thermo-mechanical analyses. However, this comes at a substantial increase in computational costs, as it is reflected by the CPU time needed to perform the analyses given in Table 2. These statements are moreover supported by the statistics of the relative difference histories given in Table 3, which additionally includes the results at the fusion line. Table 3 shows that, in general, there is an order of magnitude difference between the linear and quadratic element meshes agreement with mesh 4. In general, FAVOR is also in better agreement with mesh 4 than any of the linear meshes. For the SB-LOCA transient studied within APAL project, mesh 3q produces sufficiently accurate results as compared to FAVOR and mesh 4, the only difference being the number of elements in the cladding with respect to the latter. If the additional computational

cost involved in the use of mesh 4 is not a leading factor, this mesh could be necessary for other transients involving faster temperature fluctuations of the RPV inner surface.

Table 3: Statistics of the relative difference with respect to mesh 4 results

Statistics [%]	Mesh	$T(r_i)$	T(fl)	$S_h(r_i)$	$<S_h(fl)>$	$S_a(r_i)$	$<S_a(fl)>$
Max(abs(RD))	1	8.5E-01	2.1E+00	1.0E+01	1.5E+01	1.2E+01	1.9E+01
	2	8.5E-01	2.1E+00	1.0E+01	1.5E+01	1.2E+01	1.9E+01
	3	1.7E+00	1.9E+00	3.0E+01	1.7E+01	3.3E+01	2.5E+01
	3q	1.2E-02	1.3E-02	3.9E+00	4.1E+00	5.7E+00	5.5E+00
	FAVOR	7.5E-01	1.2E+00	5.9E+00	7.8E+00	6.5E+00	1.3E+01
Average(RD)	1	7.5E-03	4.1E-02	-3.0E+00	-7.9E+00	-4.3E+00	-8.6E+00
	2	7.4E-03	3.9E-02	-2.9E+00	-7.9E+00	-4.1E+00	-8.6E+00
	3	-2.2E-03	2.8E-02	-7.9E+00	-4.3E+00	-9.5E+00	-4.4E+00
	3q	2.1E-04	2.6E-04	-6.4E-01	1.6E-02	-1.7E+00	-5.2E-02
	FAVOR	-3.7E-03	-5.8E-01	-9.6E-01	5.7E-01	-9.6E-01	2.0E+00
STD(RD)	1	2.0E-01	3.8E-01	1.4E+00	2.8E+00	2.0E+00	3.3E+00
	2	2.0E-01	3.8E-01	1.4E+00	2.8E+00	2.0E+00	3.3E+00
	3	2.3E-01	3.6E-01	3.7E+00	2.4E+00	5.7E+00	3.3E+00
	3q	1.1E-03	1.0E-03	3.1E-01	2.8E-01	7.8E-01	3.8E-01
	FAVOR	1.0E-01	3.5E-01	1.1E+00	1.3E+00	7.4E-01	1.4E+00

Max(abs(RD)): maximum absolute value of the relative difference history
Average (RD): average value of the relative difference history
STD(RD): standard deviation of the relative difference history

5 CONCLUSIONS

This paper presents the development of a finite element model of a full 3D-RPV for future PTS analyses. Five model meshes are generated with different element densities and interpolation orders. The thermal-hydraulic results from RELAP5 code of the SB-LOCA transient are employed as inputs in the thermo-mechanical analyses with the developed RPV models. The same inputs are also employed in the FAVOR code to compare 1D and 3D RPV model results. The results of the analyses show that, although at higher computational costs, the use of quadratic elements is necessary to obtain accurate stresses. The developed quadratic meshes and FAVOR deliver very similar results. This confirms that the 1D-RPV model in FAVOR is a valid simplification of the full 3D-RPV at the middle of its cylindrical part and with a uniform-load assumption. Future work will include the 3D-RPV analyses with non-uniform thermal-hydraulic inputs.

ACKNOWLEDGMENTS

This work has been performed as a part of APAL (Advanced Pressurized Thermal Shock Analysis for Long-Term Operation) project which has received funding from the Euratom research and training programme 2019 - 2020 under grant agreement No 945253. The authors also gratefully acknowledge the financial support of the Slovenian Research Agency through the research program P2-0026. The authors would also like to show their gratitude to the APAL partners from work-packages 2 and 3 for performing the RELAP5 simulation and providing the data.

REFERENCES

[1] IAEA, "Pressurized Thermal Shock in Nuclear Power Plants: Good Practices for Assessment", IAEA-TECDOC-1627, INTERNATIONAL ATOMIC ENERGY AGENCY, 2010.
[2] C. Cueto-Felgueroso, et al., "State-of-the-art of Long-Term Operation Improvements Relevant for PTS Analysis", Structural Mechanics in Reactor Technology (SMiRT-26). IASMiRT, Berlin/Potsdam, Germany, 2022 (IN-PRESS).
[3] P. T. William, et al., Fracture Analysis of Vessels – Oak Ridge FAVOR, v16.1, Computer Code: Theory and Implementation of Algorithms, Methods, and Correlations, ORNL/LTR-2016/309, 2016.
[4] NEA/CSNI, "Comparison Report of RPV Pressurized Thermal Shock - International Comparative Assessment Study (PTS ICAS)", Nuclear Energy Agency (NEA) Commitee on the Safety of Nuclear Installations (CSNI), 1999.
[5] USNRC, RELAP5/MOD3.3 Code Manual, vol. 1-8, patch 05, Information Systems Laboratories, Inc., Rockville, MD, USA, 2016.
[6] M. Puustinen, et al., "Deliverable 2.1 - Results of TH Analysis for Selected LTO Improvements", APAL project - Advanced PTS Analysis for LTO, Euratom research and training programme 2019-2020 under grant agreement No 945253., 2022.